

^2H NMR angle-dependent spectral study of core dynamics in a discotic columnar phase

J. Zhang¹ and Ronald Y. Dong^{1,2}¹*Department of Physics and Astronomy, University of Manitoba, Winnipeg, MB, Canada R3T 2N2*²*Department of Physics and Astronomy, Brandon University, Brandon, MB, Canada R7A 6A9*

(Received 6 December 2005; published 9 June 2006)

A detailed ^2H NMR study of a discotic monomer is reported in its columnar phase at 61.4 MHz. A simulation of angular-dependent spectral patterns and/or signal intensities of the aromatic deuterons is shown to provide information on the small step (or jump) diffusion rates in the low temperature region of the D_{ho} phase, where the motion is in the intermediate motion regime. In the high end of this phase, the motion falls into the fast motion regime and spectral patterns become insensitive to the diffusion rate. In such a case, angular-dependent NMR signal intensities were used to give the required dynamic information. The diffusive motion about the columnar axis is found to be thermally activated with an activation energy of 69 kJ/mol. Deuteron spin-lattice relaxation rates were measured at 61.4 MHz and interpreted by a conventional rotational diffusion model in order to complement and compare with the above study when possible.

DOI: [10.1103/PhysRevE.73.061704](https://doi.org/10.1103/PhysRevE.73.061704)

PACS number(s): 61.30.-v

I. INTRODUCTION

Self-organizing liquid crystals (LC) formed by disk-shaped molecules [1] are of interest, since their columnar phases exhibit special anisotropic physical properties such as one-dimensional photoconductivity [2] and electron conductivity [3], etc. The disk-shaped molecules are usually composed of a rigid aromatic core surrounded by equatorial flexible chains. A large degree of conformational freedom in the “melted” hydrocarbon chains effectively decouples the ordering of the tails from the cores. There appears to be little correlation among columns (separated by ~ 2 nm), and the molecules exchange between columns at a rate of $\sim 10^5$ s⁻¹. Among discotics, those of triphenylene derivatives have been most studied, not only because their simple molecular structures allowed flexibility in the molecular engineering, but also because their aromatic cores conferred better thermal stability [4]. In the discotic columnar phase, stacks of molecular disks (separated by ~ 0.35 nm) form columns, which in turn aggregate into a two-dimensional lattice (e.g., hexagonal, or rectangular). The π^* shells of adjacent molecules in the stack tend to overlap. Because of the π overlap between the electronically active transport units, the columns provide one-dimensional pathways for charge and energy migration. One of the main factors affecting the charge transport properties of discotic materials is expected to be positional disorder, i.e., the nonparallel arrangement of disks and longitudinal and lateral displacements of molecular cores within the stacks [5]. Deviations from an ideal stacking will lead to the energy transport along the one-dimensional pathway becoming incoherent, and the transport proceeds by successive transitions from one localized site to another. In fact, the temperature-dependent disorder is related to the temperature-dependent broadening of density of states in the “hopping” model [6]. For this reason, the relation between the dynamical behaviors of the discotic LC and the understanding of the charge transport is an important issue. To this end, nuclear magnetic resonance (NMR) has been shown to be a powerful method [7] for investigating molecular dynam-

ics and ordering in columnar phases. Both order and dynamics in LC promote dynamical transport processes. The charge transport properties are potentially exploitable in applications ranging from sensing devices to high resolution xerography.

Several NMR investigations of discotic LC compounds have been reported in the literature [8–12]. ^2H NMR has often been used because of the relatively simple “planar powder” spectra observed in aligned samples of discotics. These spectra can be easily interpreted, and contain atomic resolution due to specific deuteration [13]. Aligned columnar phases can be achieved by a cooling from the isotropic phase while in a sufficiently strong magnetic field [8]. In an aligned sample, the column axis (director) is perpendicular to the magnetic field direction. The spectrum of an aligned sample at 0° orientation (i.e., the Z axis of the sample frame is along the NMR field) shows a quadrupolar doublet for each distinct deuteron. The quadrupole splitting of the aromatic deuterons gives the orientational order parameter S at different temperatures, usually ranging between 0.9 and 0.95. This reflects that the molecular cores are highly ordered in the columns. It is well known that the quadrupolar echo pulse sequence [14] $90_x^\circ - \tau - 90_y^\circ - \tau$ may produce different spectral patterns if the pulse separation τ was varied [15]. When an aligned sample is rotated from 0° to 90° in the NMR field using a goniometer probe, one can also observe different spectral patterns. If the system under study has motions in the intermediate regime (rate of the order of the interaction responsible for the observed spectral pattern), these spectral patterns contain information on the dynamic processes [16]. It is well known that ultraslow motional processes (rate less than 10^3 s⁻¹) cannot be studied by deuterium line shape analysis, while the same is true if the motional processes are fast (rate of the order of the Larmor frequency, $\sim 10^7$ s⁻¹).

Recently, dynamic information in chiral smectic phases have been derived from the angular-dependent echo intensities and spectral patterns collected at fixed τ values [17,18]. The present study exploits the same approach to gain molecular dynamic information from a triphenylene

derivative 2,7,10,11-tetrapentyloxy 3,6-diacetoxy triphenylene (HAT5a), in which two of the six pendant chains are much shorter in length [19]. The system is chosen because it shows a rather wide discotic columnar D_{ho} phase. In particular, it is expected that at the low end of this phase, molecular reorientations about the columnar axis would be in the intermediate regime, while at the high temperature region this process should likely approach the fast motion regime. In the latter regime, a more preferred technique is to measure deuteron spin-lattice relaxation rates, from which rotational diffusion constants can be derived based on a well-known motional (diffusive rotation) model [20]. In the present study, a spin relaxation technique is used to complement and contrast the technique of angular-dependent spectral patterns and echo intensities. This paper is organized as follows. Section II gives the relevant theory used to describe simulation of experimental results and to interpret the spectral densities of motion. Section III contains the experimental method, while Sec. IV gives the results and discussion. The last section gives a brief conclusion.

II. THEORY

It is known that discotic molecules possess a negative anisotropic magnetic susceptibility $\Delta\chi(=\chi_{\parallel}-\chi_{\perp})$. For a perfectly aligned sample, the directors in the columnar phase lie in a plane perpendicular to the external magnetic field, and the disk-shaped molecules can randomly reorient about their columnar axes. To study the dynamics through simulation of the experimental line shapes at different rotation angles, one may consider either a symmetric threefold jump process [21] or a planar diffusive process [22]. For threefold jumps in a plane, the molecules jump by $\pm 2\pi/3$ about their symmetry axes (which are nearly parallel to the columnar axis), while planar diffusion can be described as a reorientation mechanism via infinitesimally small steps with a diffusion constant D_R . The details of the line shape calculation based on these models are summarized in the Appendix. Here only the main results are given. The spin-lattice relaxation theory appropriate for discotics is also outlined to aid the discussion.

In aligned deuterated LC, the ^2H spin(s) gives rise to a spectrum of two lines with spectral frequencies given in the director frame (X_D, Y_D, Z_D) by [23]

$$\begin{aligned} \nu^{\pm} = & \pm \frac{3}{4} \bar{\nu}_Q \left\{ P_2(\cos \theta_0) \left[P_2(\cos \beta) + \frac{\bar{\eta}}{2} \sin^2 \beta \right] \right. \\ & + \frac{3}{4} \sin^2 \theta_0 \left[\sin^2 \beta \cos 2\alpha + \frac{\bar{\eta}}{3} (1 + \cos^2 \beta) \cos 2\alpha \right] \\ & \left. + \frac{3}{4} \sin 2\theta_0 \left[\sin 2\beta \cos \alpha - \frac{\bar{\eta}}{3} \sin 2\beta \cos \alpha \right] \right\}, \quad (1) \end{aligned}$$

where $\bar{\eta}=(\bar{V}_{XX}-\bar{V}_{YY})/\bar{V}_{ZZ}$ is a time-averaged asymmetry parameter, $\bar{\nu}_Q=eQ\bar{V}_{ZZ}/h$ is a time-averaged nuclear quadrupolar coupling constant along the director, and θ_0 is the angle between the magnetic field and the Z_S axis of the sample frame. The \bar{V}_{ii} are the principal elements of the electric field tensor in the director frame (X_D, Y_D, Z_D) . If there is no

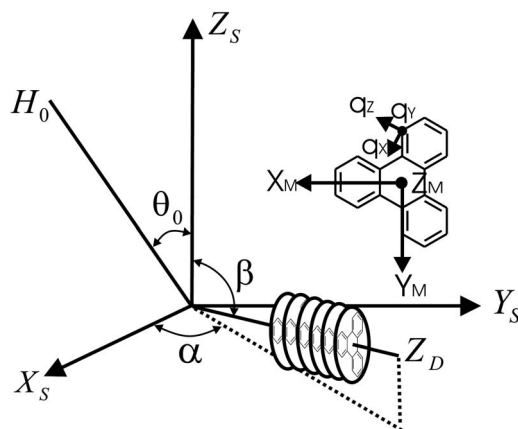


FIG. 1. Illustration of the sample frame (X_S, Y_S, Z_S) , the direction of the magnetic field, H_0 , the direction of the director, Z_D , the molecular frame (X_M, Y_M, Z_M) , and the principal axis frame of the electric field gradient (q_X, q_Y, q_Z) . The Euler angles for the coordinate transformation from (X_M, Y_M, Z_M) to (q_X, q_Y, q_Z) are $(\phi, \pi/2, \pi/2)$.

sample rotation, θ_0 will be 0. $(\alpha, \beta, 0)$ are the Euler angles that give the orientation of the director in the sample frame (X_S, Y_S, Z_S) (Fig. 1). To analyze the effect of rotational diffusion or jump on the observed deuteron spectra, one needs to introduce a molecular frame. The Euler angles for coordinate transformation from the director frame (X_D, Y_D, Z_D) to the molecular frame (X_M, Y_M, Z_M) are $(0, \theta, 0)$, and $(\phi, \pi/2, \pi/2)$ for a transformation from (X_M, Y_M, Z_M) to the C-D bond frame (q_X, q_Y, q_Z) . Figure 1 shows the relevant coordinate systems and the Euler angles describing transformations between them. Since

$$\begin{aligned} \bar{V}_{ZZ} = & \sqrt{\frac{2}{3}} \langle R_{2,0}^D \rangle = -\frac{1}{2} e q \left[\langle P_2(\cos \theta) \rangle (1 + \eta) \right. \\ & \left. - \frac{3 - \eta}{2} \overline{\cos 2\phi} \langle \sin^2 \theta \rangle \right], \\ \bar{V}_{XX} - \bar{V}_{YY} = & \langle R_{2,2}^D \rangle + \langle R_{2,-2}^D \rangle \\ = & -\frac{3}{4} \langle \sin^2 \theta \rangle e q (1 + \eta) + \frac{1}{4} (1 \\ & + \langle \cos^2 \theta \rangle) e q \overline{\cos 2\phi} (3 - \eta), \quad (2) \end{aligned}$$

one obtains when θ is small,

$$\bar{\nu}_Q = -\frac{q_{CD}}{2} (1 + \eta) S, \quad \bar{\eta} = -\frac{(3 - \eta) \overline{\cos 2\phi}}{(1 + \eta) S}, \quad (3)$$

where $S = \langle P_2(\cos \theta) \rangle$ is the orientational order parameter of the molecule, $q_{CD} = \frac{e^2 Q q}{h}$ and η is the asymmetry parameter of a nuclear quadrupole interaction. From the quadrupolar splitting, S can be calculated to a first approximation [$\bar{\eta}=0$ in Eq. (1)] using

$$\Delta\nu = \frac{3}{8} q_{CD} (1 + \eta) S. \quad (4)$$

To obtain the time-domain free induction decay (FID) signal, one needs to solve the equation of motion [24]

$$\frac{d}{dt}\mathbf{G}(\phi, t) = -\mathbf{R}\mathbf{G}(\phi, t), \quad (5)$$

where $\mathbf{G}(\phi, t)$ is magnetization from the molecule with a particular ϕ orientation and \mathbf{R} is the jump (or diffusive) matrix which describes the reorientation process (see the Appendix). The magnetization [25] obtained after a quadrupole echo pulse sequence is

$$\mathbf{G}(\phi, t) = e^{-\mathbf{R}(\tau+t)}[e^{-\mathbf{R}\tau}\mathbf{G}(0)]^*. \quad (6)$$

The overall time-domain FID signal F is obtained by integrating over α and β :

$$F(\theta_0, t) = \int_{(\pi/2)-3\sigma}^{(\pi/2)+3\sigma} \int_0^{2\pi} F(\theta_0, \alpha, \beta, t) \left[\frac{1}{\sqrt{2\pi\sigma}} \times e^{-(\beta - \pi/2)^2/2\sigma^2} \right] e^{-\Sigma^2 t^2/2} \sin \beta d\alpha d\beta, \quad (7)$$

where $F(\theta_0, \alpha, \beta, t)$ is related to $\mathbf{G}(\phi, t)$ as described in the Appendix. $e^{-\Sigma^2 t^2/2}$ is used to account for the observed line broadening, which is controlled by a fitting parameter Σ . Although the sample is aligned, the directors do not in practice all lie perfectly on a plane perpendicular to the magnetic field, but are distributed around it. In this equation a Gaussian distribution has been assumed with a characteristic width σ . The absorption spectrum is proportional to the Fourier transform of the FID signal:

$$S(\theta_0, 2\tau) = \int_0^\infty F(\theta_0, t) e^{-i\omega t} dt. \quad (8)$$

By line shape simulation, the jump rate K_J or diffusion constant D_R can be obtained. An alternative method is to fit the quadrupole echo intensity as a function of a sample rotation angle by using Eq. (7) at $t=0$. Here, a minimization routine can be used to minimize the sum-squared error f :

$$f = \sum_m [I^{expt}(\theta_0, 2\tau) - I^{calc}(\theta_0, 2\tau)]_m^2, \quad (9)$$

where m is the number of different θ_0 and the superscripts *expt* and *calc* denote experimental and calculated, respectively. $I^{calc}(\theta_0, 2\tau)$ is given by Eq. (7) with $t=0$. The best fit allows the determination of K_J or D_R . This method is necessary when the motional rates are $\geq 10^7$ s⁻¹.

For deuteron spin(s), the standard spin relaxation theory gives two spin-lattice relaxation times. One is for the Zeeman order T_{1Z} and the other is for the quadrupolar order T_{1Q} . For the director oriented at $\beta=90^\circ$ with respect to the magnetic field (in our aligned sample), the relaxation rates are given in terms of the spectral densities $J_m(mw_0, \beta)$ [13]:

$$T_{1Q}^{-1} = 3J_1(w_0, 90^\circ),$$

$$T_{1Z}^{-1} = J_1(w_0, 90^\circ) + 4J_2(2w_0, 90^\circ), \quad (10)$$

where $w_0/2\pi$ is the Larmor frequency. The above measured spectral densities can be written in terms of $J_m(w, 0^\circ) = J_m(w)$, $m=0, 1, 2$, for the director aligned along the external magnetic field, as follows [13]:

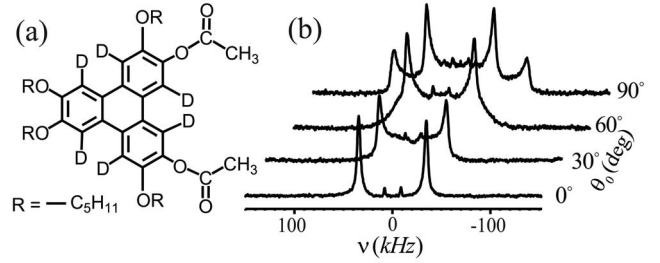


FIG. 2. (a) Molecular structure of a core deuterated HAT5a-d₆. (b) Typical ²H NMR spectra collected at different θ_0 values with $\tau=30$ μ s and at $T=367$ K.

$$J_1(w, 90^\circ) = \frac{1}{2}[J_1(w) + J_2(w)],$$

$$J_2(2w, 90^\circ) = \frac{3}{8}J_0(2w) + \frac{1}{2}J_1(2w) + \frac{1}{8}J_2(2w). \quad (11)$$

The spectral densities $J_m(w)$ reflect the nature of the molecular motion which induces the nuclear spin relaxation. It is well established [12] that for discotic mesogens, molecular reorientations can be satisfactorily described by the anisotropic viscosity model (AVM) [20]. In the anisotropic viscosity model, one needs to solve the rotational diffusion equation

$$\frac{\partial}{\partial t}P(\Omega, t) = \Gamma_\Omega P(\Omega, t), \quad (12)$$

where the diffusion operator Γ_Ω contains the potential of the mean torque $U(\Omega)$, the rotational diffusion tensor \mathbf{D} , and $P(\Omega, t)$ is the probability of finding a molecule with the orientation Ω at time t . At each temperature, the mean potential is specified by the S value. In particular, the tensor \mathbf{D} is diagonalized in the director frame. If the molecular Z_M axis is taken to be close to the mesophase director (due to $S \approx 1$), Γ_Ω involves derivatives with respect to Euler angles α' and β' , and the diffusion tensor \mathbf{D} has two principal elements $D_{\alpha'}$ and $D_{\beta'}$ in the director frame [20]. The diffusion constants $D_{\alpha'}$ and $D_{\beta'}$ are for diffusive rotations of the molecule about the director axis, and for rotations away or towards the director, respectively. The spectral densities $J_m(w)$ for the ring deuterons can be obtained by the Fourier transform of the correlation functions. In the notation given in Ref. [26]

$$J_n(w) = \frac{3\pi^2}{2} q_{CD}^2 \sum_m [d_{m0}^2(\beta_{M,Q})]^2 \sum_K \frac{(\beta_{mn}^2)_K (\alpha_{mn}^2)_K}{(\alpha_{mn}^2)_K + w^2}, \quad (13)$$

where $q_{CD}=185$ KHz, $\beta_{M,Q}=90^\circ$ is the angle between the C-D bond and the molecular Z_M axis. $(\alpha_{mn}^2)_K/D_{\beta'}$, and $(\beta_{mn}^2)_K$ are the eigenvalues and eigenvectors obtained from diagonalizing the diffusion operator matrix. Note that $D_{\alpha'}$ and $D_{\beta'}$ appear in $(\alpha_{mn}^2)_K$.

III. EXPERIMENT

A core deuterated sample of 2,7,10,11-tetrapentyloxy 3,6-diacetoxy triphenylene (HAT5a-d₆) is shown in Fig. 2(a).

The reported transition temperature between the D_{ho} and isotropic phase of a protonated HAT5a sample is 442 K [19]. This transition temperature was estimated at 438 ± 2 K in our deuterated sample based on the NMR spectra. The uncertainty is mainly due to a significant biphasic region. The sample was aligned by cooling slowly from the isotropic phase to the desired temperature in the D_{ho} phase. The deuterium spectral patterns were taken using a Bruker goniometer probe equipped with a high precision pneumatic motor, giving an angular resolution of 0.1° , and a Bruker Avance 400 solid state system. The NMR magnetic field was 9.4 T and the deuteron Larmor frequency was 61.4 MHz. The sample temperature was controlled by an air flow and the temperature gradient across the sample was estimated to be better than 0.5° . A quadrupole echo pulse sequence was used to generate ^2H spectra, and to give the echo maximum intensities at different rotation angles. The 90° pulse width was $2.6 \mu\text{s}$. The number of scans needed to observe the FID or its Fourier transform depends on the temperature. When the temperature was lowered, the number of scans was increased to achieve a good signal. The recycle time between scans was 0.3 s. In the low temperature range, our experiments did not show any observable field-induced sample reorientation and columnar destruction in the studied θ_0 region of 0° – 90° . However, at high temperatures, the FID intensities at high sample rotation angles ($>50^\circ$) did show considerable deviations from predictions of the theoretical model. This is perhaps due partly to a small amount of impurity in the sample and partly to the magnetic torque on the molecules. At high sample rotation angles, the director(s) tends to reorient by the magnetic torque due to the NMR field. The director reorientation is particularly easy at high temperatures where viscosities are lower. Figure 2(b) shows some typical spectra at $T=367$ K for different rotation angles. There was a dramatic spectral change when the sample was rotated from 0° to 90° . Most spectra exhibit a small doublet, likely caused by a small amount of impurity in the sample. When the sample temperature was lowered, the intensity of the impurity doublet tended to increase. But this signal did not affect our line shape simulation. The T_{1Z} and T_{1Q} measurements were simultaneously collected in the temperature range up to ~ 393 K using a broadband Jeener-Broekaert sequence [27]. Signal averaging required 1024 scans. No attempt was made to measure T_{1s} at higher temperatures, partly due to the fear of further sample degradation and partly due to temperature instability in our probe. The accuracy of spin relaxation measurements was estimated to be better than 5%.

IV. RESULTS AND DISCUSSION

The quadrupolar splitting of the aromatic deuterons in HAT5a- d_6 is plotted versus temperature in Fig. 3. From the quadrupolar splitting, S can be calculated using Eq. (4) (Table I). To obtain the dynamic parameters for the molecular motion, the threefold jump model and planar diffusion model (PDM) are compared in the Appendix. The line shapes calculated by these two models are quite similar and it is hard to tell which model (jump or diffusion) is good or better

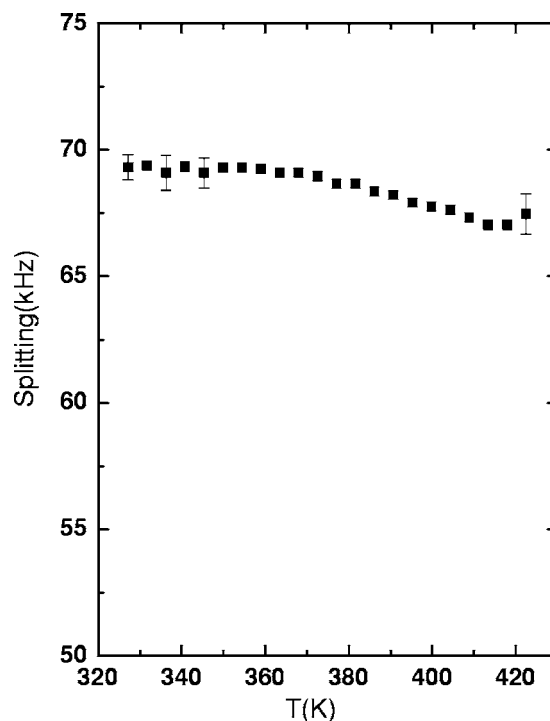


FIG. 3. Plot of the quadrupolar splitting versus the temperature for HAT5a- d_6 .

[22]. We therefore present the results based on the planar diffusion model, partly due to the treatment of relaxation data afforded by the AVM.

A. Study of the intermediate motion regime

Typical ^2H NMR spectra collected with $\tau=30 \mu\text{s}$ at different θ_0 for three temperatures are shown in Fig. 4. The simulated spectra for these temperatures are also shown. The same set of simulation parameters [Eq. (7)] was used for all rotation angles. These are listed in Table I. In the simulation, best results were obtained using $\Sigma=15$ kHz and $\eta=0.064$. To get quantitative information, the diffusion parameter D_R is varied to match the observed line shapes with the simulated

TABLE I. Parameters used in the simulation of experimental NMR spectra of HAT5a- d_6 .

Temp. (K)	D_R (rad^2/s)	S	σ (deg)	$1/T_2$ (kHz)
332	$(1.5 \pm 0.1) \times 10^6$	0.956 ± 0.005	9 ± 1	4
337	$(2.3 \pm 0.1) \times 10^6$	0.954 ± 0.005	9 ± 1	4
342	$(2.8 \pm 0.1) \times 10^6$	0.952 ± 0.005	9 ± 1	1
347	$(5.0 \pm 0.1) \times 10^6$	0.948 ± 0.005	9 ± 1	1
352 ^a	$(7.3 \pm 0.1) \times 10^6$	0.945 ± 0.005	11 ± 1	0.1
357 ^a	$(9.7 \pm 0.1) \times 10^6$	0.941 ± 0.005	11 ± 1	0.1
362	$(1.3 \pm 0.1) \times 10^7$	0.939 ± 0.005	9 ± 1	—
367	$(1.5 \pm 0.1) \times 10^7$	0.937 ± 0.005	9 ± 1	—

^aFitting parameters for both line shape and FID intensity (T_2 is not used).

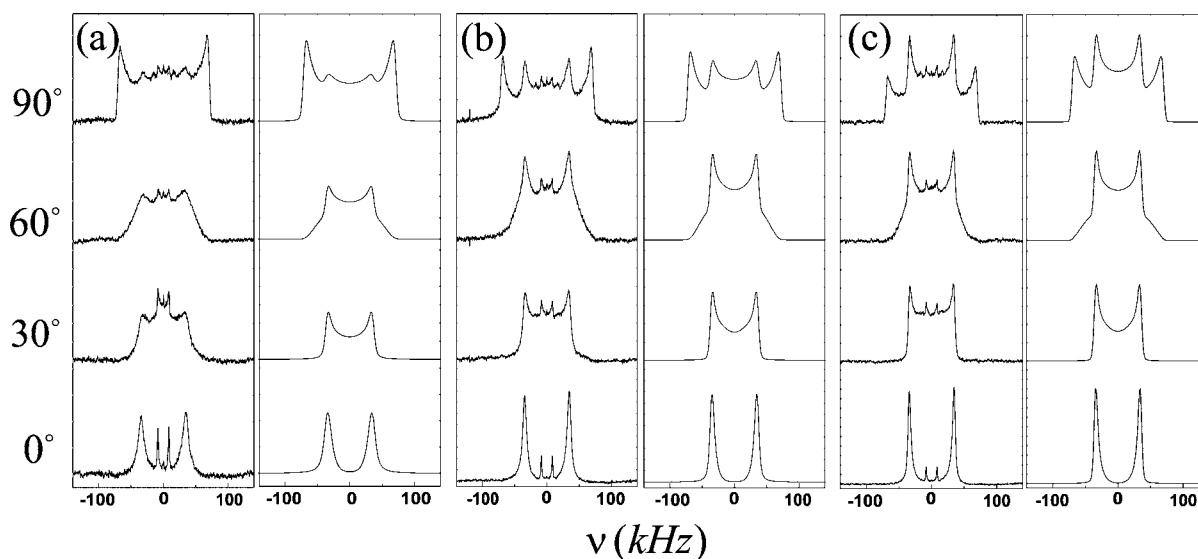


FIG. 4. Experimental (left) and corresponding calculated (right) ^2H NMR spectra for different θ_0 at 337 K (a), 347 K (b) and 357 K (c) using planar diffusion model.

spectra at different rotation angles. The line shape at $\theta_0 = 90^\circ$ tends to control the D_R value, and this is particularly true at high temperatures (e.g., see the 357 K spectrum in Fig. 4).

As mentioned before, when the temperature increases, the molecular motion becomes faster ($D_R \geq 10^7 \text{ rad}^2/\text{s}$). As a consequence, the line shape simulation is unable to give a reliable D_R value (i.e., to achieve a good fit of 90° spectral pattern, D_R tends to be driven to higher values). As seen in Fig. 4, the powder spectral line shape at $\theta_0 = 90^\circ$ and 357 K could not be reproduced faithfully with the D_R value of $9.7 \times 10^6 \text{ rad}^2/\text{s}$. Instead, a D_R value of $1.7 \times 10^7 \text{ rad}^2/\text{s}$ would fit it better, while not affecting those at low angles. Hence an angular-dependent study of the echo intensity is adopted. To demonstrate this method and to extract the diffusion constant from the intensities, Fig. 5 shows the normalized intensity $I(\theta_0, 2\tau)/I(\theta_0, 2\tau)_{\max}$ versus the rotation angle ($0^\circ - 50^\circ$) for

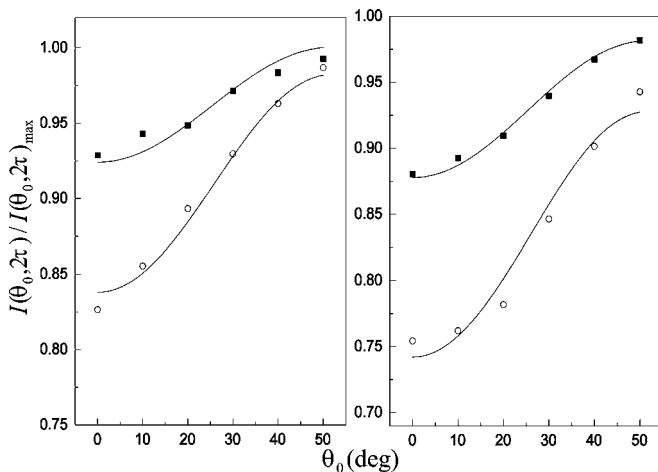


FIG. 5. Experimental and calculated normalized echo intensity $I(\theta_0, 2\tau)/I(\theta_0, 2\tau)_{\max}$ at $T = 367 \text{ K}$ (left) and $T = 357 \text{ K}$ (right) with $\tau = 15 \mu\text{s}$ (■) and $\tau = 30 \mu\text{s}$ (○).

two different τ values at two temperatures. The fitting parameters are also given in Table I. The σ values seem to be independent of the temperature. The diffusion constant D_R is plotted versus the reciprocal temperature in Fig. 6 to demonstrate that the reorientation process is thermally activated. From $D_R = D_R^0 \exp[-E_a/RT]$, the activation energy $E_a = 69 \pm 3 \text{ kJ/mol}$ is found. This value is consistent with the results of the relaxation study of similar monomers [9,12].

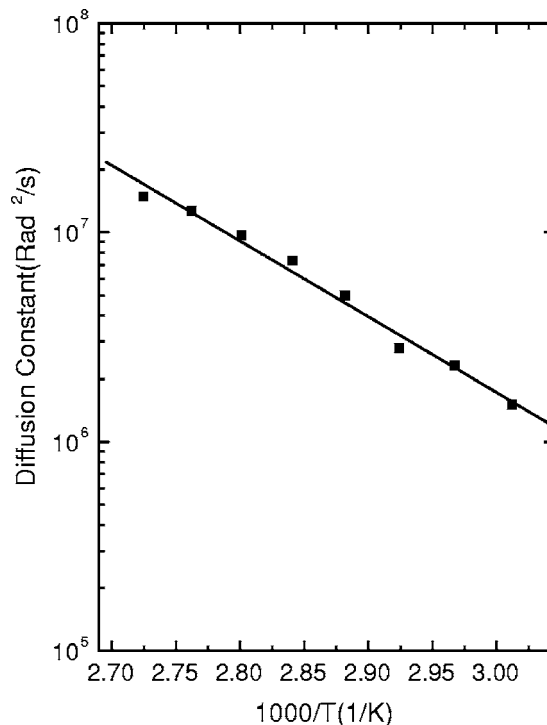


FIG. 6. Plot of the planar diffusion constant D_R versus the reciprocal temperature for HAT5a-d₆.

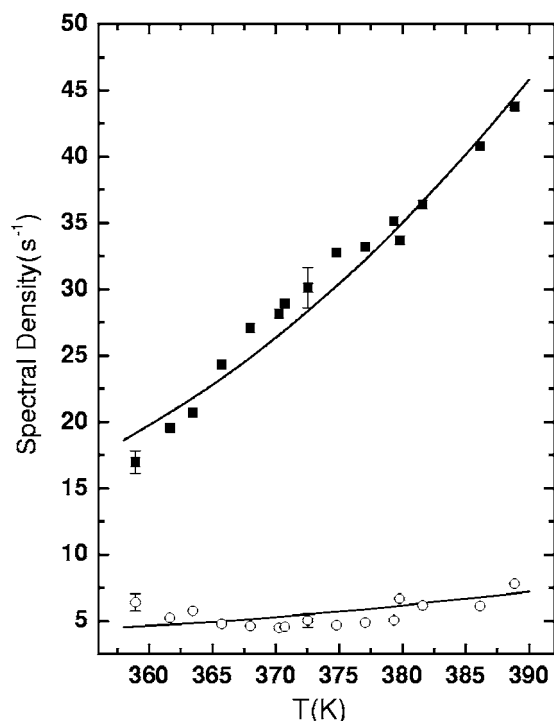


FIG. 7. Plot of spectral densities $J_1(w_0, 90^\circ)$ (■) and $J_2(2w_0, 90^\circ)$ (○) versus the temperature for HAT5a-d₆. Solid curves represent calculated spectral densities based on an anisotropic viscosity model.

B. Study of the fast motion regime

In the high temperature region, the molecular motion will be fast, and one cannot get molecular dynamic information by only fitting the FID intensity and spectral line shape. To complement the above study, the spin-lattice relaxation technique is adopted to study dynamics at high temperatures. The spectral densities $J_1(w_0, 90^\circ)$ and $J_2(2w_0, 90^\circ)$ derived from the deuteron spin-lattice relaxation rates in Eq. (10) are plotted as a function of temperature in Fig. 7. By using the AVM, the spectral densities can be calculated from Eqs. (11) and (13). A minimization (AMOEBA) routine was used to minimize the sum-squared error e :

$$e = \sum_k \sum_m [J_m^{calc}(mw_0, 90^\circ) - J_m^{exp}(mw_0, 90^\circ)]_k^2, \quad (14)$$

where the sum over k is for nine temperatures, $m=1$ or 2 . A global target method was carried out by assuming Arrhenius-type relations: $D_{\alpha'} = D_{\alpha'}^0 \exp[-E_{\alpha'}^a/RT]$ and $D_{\beta'} = D_{\beta'}^0 \exp[-E_{\beta'}^a/RT]$. The fittings are good and the derived diffusion constants $D_{\alpha'}$ and $D_{\beta'}$ are plotted in Fig. 8. The activation energy for the α' motion $E_{\alpha'}^a \approx 6.0$ kJ/mol and for β' motion $E_{\beta'}^a \approx 31.8$ kJ/mol. These activation energies appear to be low in comparison with those found in similar compounds [12], most likely due to the unavailability of relaxation measurements at another Larmor frequency.

Comparing the results of diffusion constants at the same temperature derived from two different models (PDM and AVM), we find that $D_{\beta'} < D_R < D_{\alpha'}$. This seems reasonable because in the AVM two parameters $D_{\alpha'}$ and $D_{\beta'}$ are used to

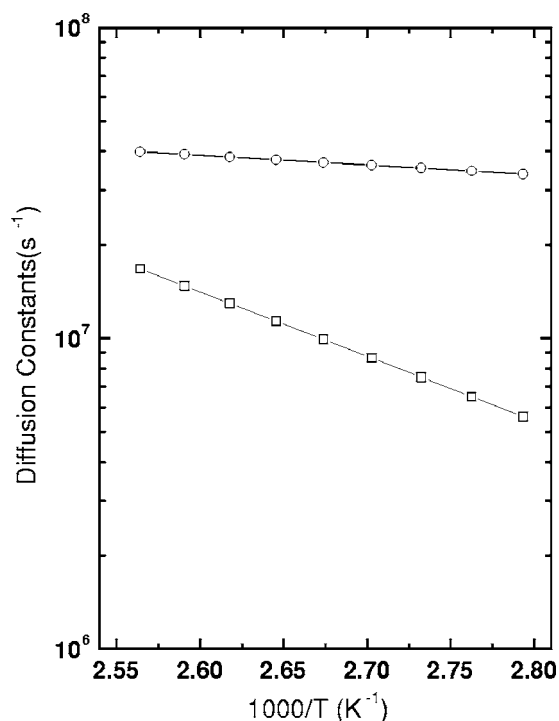


FIG. 8. Plot of rotational diffusion constants $D_{\alpha'}$ (—○—) and $D_{\beta'}$ (—□—) versus the reciprocal temperature for HAT5a-d₆.

describe the molecular motion: diffusive precession motion and libration motion of the molecular plane, while in the PDM only D_R is used to describe the “planar” rotational diffusive motion, which should mimic the combined effect of the α' and β' motion. However, it is noticed that the activation energy obtained from PDM is larger than those in AVM. We believe that the activation energy of D_R from PDM is likely more correct, since the activation energies found from the AVM are based on data collected at a single Larmor frequency.

V. CONCLUSION

In summary, the present study has combined nuclear spin relaxation and dynamic NMR spectroscopy to study axial motions of a discotic monomer with dissimilar side chains as a function of temperature in the columnar D_{ho} phase. The motional parameters derived from the two approaches are compared. In particular, the present study has demonstrated that angular-dependent echo intensities at fixed τ in a quadrupolar echo experiment can be particularly sensitive in pinning down the rate process when this rate approaches the fast motion regime. The spinning motion of the molecular core is found at a rate of $\sim 10^7$ s⁻¹ in HAT5a. This number is significantly lower than the typical “hopping” rate of electrons/holes (10^{10} s⁻¹) in discotic LC. Thus, the dynamic disorder in the columnar phases appears to be static as far as charge transport process is concerned. The potential of applying the present methodology to study dimeric discotics is real, especially when the sample alignment cannot be easily achieved in an external magnetic field.

ACKNOWLEDGMENTS

The financial support of the Natural Sciences and Engineering Council of Canada, Canada Foundation of Innovation, and Brandon University are gratefully acknowledged. R.Y.D thanks H.W. Spiess and M. Werth, Mainz for the use of deuteriated HAT5a sample.

APPENDIX A

1. Threefold jump model

In the threefold jump mechanism [24], the magnetizations $G(\phi, t)$, $G(\phi+2\pi/3, t)$, $G(\phi-2\pi/3, t)$ are coupled by the jump process with the jump matrix

$$\mathbf{R} = \begin{pmatrix} i2\pi\nu(\phi) + 2K_J + \frac{1}{T_2} & -K_J & -K_J \\ -K_J & i2\pi\nu(\phi + \frac{2}{3}\pi) + 2K_J + \frac{1}{T_2} & -K_J \\ -K_J & -K_J & i2\pi\nu(\phi - \frac{2}{3}\pi) + 2K_J + \frac{1}{T_2} \end{pmatrix}, \quad (\text{A1})$$

where K_J is the jump rate and $1/T_2$ is an exchange independent relaxation term. The echo intensity for certain θ_0 , α , β , and ϕ is computed by summing over all components G_i [using Eq. (6)], $F(\theta_0, \alpha, \beta, \phi, t) = \text{Re}\{\mathbf{1} \cdot \mathbf{G}\}$ for a ϕ angle, and $F(\theta_0, \alpha, \beta, t) = \int_0^{2\pi} F(\theta_0, \alpha, \beta, \phi, t) d\phi$. In practice, the integration was performed by summing over ϕ and α at intervals of 2.8° and summing over β at intervals of 3° between $\frac{\pi}{2} - 3\sigma$ and $\frac{\pi}{2} + 3\sigma$. The simulated spectrum is obtained by using Eqs. (7) and (8) in the main text.

2. Planar diffusion model

For the random planar diffusive motion [24], the diffusion operator is

$$\Gamma_\phi = D_R \frac{\partial^2}{\partial \phi^2}. \quad (\text{A2})$$

Then the transverse magnetization obeys the equation of motion

$$\frac{d}{dt} G(\phi, t) = \left[-i w_Q(\phi) - 1/T_2 + D_R \frac{\partial^2}{\partial \phi^2} \right] G(\phi, t), \quad (\text{A3})$$

where w_Q can be expanded as a series of $e^{in\phi}$ [22]

$$w_Q(\phi) = 2\pi\nu_Q(\phi) = A + B(e^{i\phi} + e^{-i\phi}) + C(e^{i2\phi} + e^{-i2\phi}) \quad (\text{A4})$$

with

$$A = -\frac{3}{4}\pi\nu_Q(1 + \eta)S\{P_2(\cos \theta_0)P_2(\cos \beta) + \frac{3}{4}\sin^2 \theta_0 \sin^2 \beta \cos 2\alpha + \frac{3}{4}\sin 2\theta_0 \sin 2\beta \cos \alpha\},$$

$$B = 0,$$

$$C = \frac{3}{8}\pi\nu_Q(3 - \eta)\left\{\frac{1}{2}P_2(\cos \theta_0)\sin^2 \beta + \frac{1}{4}\sin^2 \theta_0(1 + \cos^2 \beta)\cos 2\alpha - \frac{1}{4}\sin 2\theta_0 \sin 2\beta \cos \alpha\right\}. \quad (\text{A5})$$

Here B is zero since the aromatic C-D bond is orthogonal to the planar normal of the disklike molecule. The FID signal is proportional to the real part of the integral over $G(\phi, t)$:

$$F(\theta_0, \alpha, \beta, t) \propto \text{Re} \int_0^{2\pi} d\phi G(\phi, t). \quad (\text{A6})$$

To solve $G(\phi, t)$, it is expanded in a complete set of exponential functions [22]:

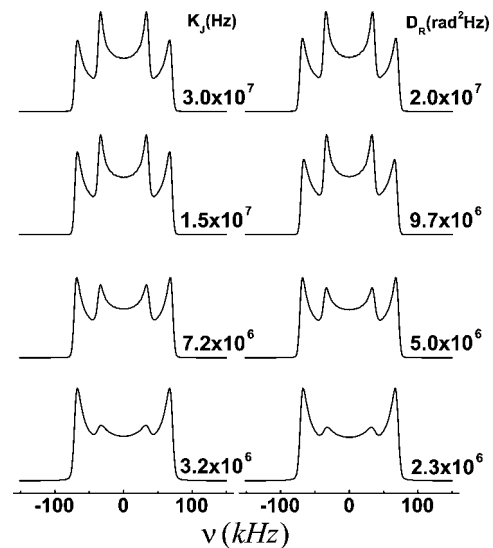


FIG. 9. Comparison of simulated spectra at $\theta_0=90^\circ$ calculated for the threefold jump model (left) and the planar diffusion model (right).

$$G(\phi, t) = \sum_{k'=-\infty}^{\infty} a_{k'}(t) \exp(ik' \phi). \quad (\text{A7})$$

Substituting (A7) and (A4) into (A3), and multiplying by $\exp(-ik\phi)$, one gets, after integrating over ϕ

$$\begin{aligned} \frac{da_k(t)}{dt} = & - \left[iA + \frac{1}{T_2} + k^2 D_R \right] a_k(t) - iB[a_{k+1}(t) + a_{k-1}(t)] \\ & - iC[a_{k+2}(t) + a_{k-2}(t)]. \end{aligned} \quad (\text{A8})$$

By adding the equations for $a_k(t)$ and $a_{-k}(t)$ and by defining

$$\bar{a}_0(t) = \sqrt{2}a_0(t),$$

$$\bar{a}_k(t) = a_k(t) + a_{-k}(t), \quad k \neq 0, \quad (\text{A9})$$

Eq. (A8) can be written as

$$\frac{d\bar{\mathbf{a}}(t)}{dt} = -\mathbf{R}\bar{\mathbf{a}}(t) \quad (\text{A10})$$

or

$$\frac{d}{dt} \begin{pmatrix} \bar{a}_0(t) \\ \bar{a}_1(t) \\ \bar{a}_2(t) \\ \vdots \\ \bar{a}_k(t) \end{pmatrix} = - \begin{pmatrix} iA + \frac{1}{T_2} & 0 & i\sqrt{2}C & & \\ 0 & iA + \frac{1}{T_2} + D_R + iC & 0 & iC & \\ i\sqrt{2}C & 0 & iA + \frac{1}{T_2} + 4D_R & 0 & iC \\ & & & \ddots & \\ iC & 0 & & & iA + \frac{1}{T_2} + k^2 D_R \end{pmatrix} \begin{pmatrix} \bar{a}_0(t) \\ \bar{a}_1(t) \\ \bar{a}_2(t) \\ \vdots \\ \bar{a}_k(t) \end{pmatrix}. \quad (\text{A11})$$

To find $\bar{\mathbf{a}}(t)$, the matrix \mathbf{R} can be truncated at some sufficiently high k value (in our study, $k=6$ suffices). For the quadrupole echo experiment,

$$\begin{aligned} \bar{\mathbf{a}}(t) &= \exp[-\mathbf{R}(\tau+t)] \exp[-\mathbf{R}\tau]^* \bar{\mathbf{a}}(0) \\ &= [T e^{-\Lambda(t+\tau)} T^{-1}] [T e^{-\Lambda\tau} T^{-1}]^* \bar{\mathbf{a}}(0), \end{aligned} \quad (\text{A12})$$

where T is a unitary matrix which diagonalizes \mathbf{R} to give a diagonal matrix Λ of its eigenvalues, λ_j . When $t=0$, $G(\phi, 0)=1$ and is independent on ϕ . Then $\bar{a}_k(0)=0, k \neq 0$ and $\bar{a}_0(0)=1$. Thus, one has

$$F(\theta_0, \alpha, \beta, t) = \mathbf{1} \cdot \bar{\mathbf{a}}(t). \quad (\text{A13})$$

After $F(\theta_0, \alpha, \beta, t)$ is obtained, Eqs. (7) and (8) can be used to get the spectrum. We note that in this case, the computation time is much reduced, because there is no integration

over the angle ϕ in the simulation. The integration is still needed over angles α and β as before.

3. Comparison of threefold jump model and PDM

In the simulation, both the threefold jump model and the planar diffusion model were used to fit the line shape. Since the spectrum at $\theta_0=90^\circ$ is sensitive to K_J or D_R , we calculate the spectra based on these two models at this angle, as shown in Fig. 9. It may be seen that the pairwise matching of the spectra is obtained for $K_J/D_R \approx 1.3-1.5$, so that if one prefers to interpret the spectra in the main text by the threefold jump model, the K_J may be found by scaling accordingly. It is also demonstrated that in the fast motion limit ($K_J \geq 1.5 \times 10^7/s$ or $D_R \geq 1.0 \times 10^7 \text{ rad}^2/s$), the line shape will not change regardless of either model.

[1] C. Destrade, N. H. Tinh, and H. Gasparoux, *Mol. Cryst. Liq. Cryst.* **71**, 111 (1981).
 [2] D. Adam, F. Closs, T. Frey, D. Funhoff, D. Haarer, H. Ringsdorf, P. Schuhmacher, and K. Siemensmeyer, *Phys. Rev. Lett.* **70**, 457 (1993).
 [3] N. Boden, R. J. Bushby, and J. Clements, *J. Phys. Chem.* **98**, 5920 (1993).
 [4] D. Markovitsi, A. Germain, P. Millie, P. Lecuyer, L. K. Gallo,

P. Argyrakis, H. Bengs, and H. Ringsdorf, *J. Phys. Chem.* **99**, 1005 (1995).
 [5] A. M. de Craats, L. D. A. Siebbeles, I. Bleyl, D. Haarer, Y. A. Berlin, A. A. Zharikov, and J. M. Warman, *J. Phys. Chem. B* **102**, 9625 (1998).
 [6] H. Bassler, *Adv. Mater. (Weinheim, Ger.)* **5**, 662 (1993).
 [7] R. Y. Dong, *Annu. Rep. NMR Spectrosc.* **53**, 67 (2004).
 [8] D. Goldfarb, Z. Luz, and H. Zimmermann, *J. Phys. (Paris)* **42**,

- 1303 (1981).
- [9] X. Shen, R. Y. Dong, N. Boden, R. J. Bushby, P. S. Martin, and A. Wood, *Phys. Rev. E* **108**, 4324 (1998).
- [10] N. Boden, R. J. Bushby, C. Hardy, and F. Sixl, *J. Chem. Phys.* **123**, 359 (1986).
- [11] S. V. Dvinskikh, I. Furo, H. Zimmermann, and A. Maliniak, *Phys. Rev. E* **65**, 050702(R) (2002).
- [12] R. Y. Dong, N. Boden, R. J. Bushby, and P. Martin, *Mol. Phys.* **97**, 1165 (1999).
- [13] R. Y. Dong, *Nuclear Magnetic Resonance of Liquid Crystals* (Springer-Verlag, New York, 1997).
- [14] J. H. Davis, K. R. Jeffrey, M. Bloom, M. I. Valic, and T. P. Higgs, *Chem. Phys. Lett.* **42**, 390 (1976).
- [15] H. W. Spiess and H. Sillescu, *J. Magn. Reson. (1969-1992)* **42**, 381 (1981).
- [16] Z. Luz, in *NMR of Ordered Liquids*, edited by E. E. Burnell and C. A. de Lange (Kluwer Academic Publishers, Netherlands, 2003).
- [17] J. Xu, C. A. Veracini, and R. Y. Dong, *Phys. Rev. E* **72**, 051703 (2005).
- [18] J. Xu, C. A. Veracini, and R. Y. Dong, *Phys. Rev. E* **73**, 011705 (2006).
- [19] W. Kranig, B. Huser, H. W. Spiess, H. R. W. Kreuder, and H. Zimmermann, *Adv. Mater. (Weinheim, Ger.)* **2**, 36 (1990).
- [20] C. F. Polnaszek, G. V. Bruno, and J. H. Freed, *J. Chem. Phys.* **58**, 3185 (1973).
- [21] S. Zamir, R. Poupko, Z. Luz, and S. Alexander, *J. Chem. Phys.* **94**, 5939 (1991).
- [22] R. Poupko, Z. Luz, N. Spielberg, and H. Zimmermann, *J. Am. Chem. Soc.* **111**, 6094 (1989).
- [23] M. J. Vaz, Z. Yaniv, R. Y. Dong, and J. W. Doane, *J. Magn. Reson. (1969-1992)* **62**, 461 (1985).
- [24] S. Zamir, Z. Luz, R. Poupko, S. Alexander, and H. Zimmermann, *J. Chem. Phys.* **94**, 5927 (1991).
- [25] A. J. Vega and Z. Luz, *J. Chem. Phys.* **86**, 1803 (1987).
- [26] R. Tarroni and C. Zannoni, *J. Chem. Phys.* **95**, 4550 (1991).
- [27] S. Wimperis, *J. Magn. Reson. (1969-1992)* **86**, 46 (1973).